

Proposal to the ISOLDE and Neutron time-of-flight  
Experiments Committee

**Measurements of Fission Cross Sections of Actinides**

*The n\_TOF Collaboration(\*)*

Spokespersons: C Stephan, P Cennini  
Technical Co-ordinator & GLIMOS: P Cennini

**Abstract**

A measurement of the neutron induced fission cross sections of  $^{237}\text{Np}$ ,  $^{241,243}\text{Am}$  and of  $^{245}\text{Cm}$  is proposed for the n\_TOF neutron beam. Two sets of fission detectors will be used: one based on PPAC counters and another based on a fast ionization chamber (FIC). A total of  $5 \times 10^{18}$  protons are requested for the entire fission measurement campaign.

## (\*)LIST OF AUTHORS

U. Abbondanno<sup>1</sup>, G. Aerts<sup>2</sup>, H. Alvarez<sup>3</sup>, S. Andriamonje<sup>2</sup>, A. Angelopoulos<sup>4</sup>,  
P. Assimakopoulos<sup>4</sup>, C. O. Bacri<sup>5</sup>, G. Badurek<sup>6</sup>, P. Baumann<sup>28</sup>, F. Becvar<sup>7</sup>, H. Beer<sup>8</sup>, J. Benlliure<sup>3</sup>,  
B. Berthier<sup>5</sup>, E. Berthoumieux<sup>2</sup>, J. P. Bertuzzi<sup>9</sup>, D. Blanc<sup>9</sup>, R. Bonzano<sup>9</sup>, C. Borcea<sup>9</sup>, P. Bourquin<sup>9</sup>,  
N. Bustreo<sup>10</sup>, J. Buttkus<sup>9</sup>, F. Calvino<sup>11</sup>, D. Cano-Ott<sup>12</sup>, R. Capote<sup>13</sup>, R. Cappi<sup>9</sup>, J. C. Carlier<sup>9</sup>, P.  
Carlson<sup>14</sup>, E. Cennini<sup>9</sup>, P. Cennini<sup>9</sup>, D. Chapuis<sup>9</sup>, V. Chepel<sup>15</sup>, E. Chiaveri<sup>9</sup>, V. Chohan<sup>9</sup>, C.  
Coceva<sup>16</sup>, N. Colonna<sup>17</sup>, J. P. Come<sup>9</sup>, G. Cortes<sup>11</sup>, D. Cortina<sup>3</sup>, A. Couture<sup>18</sup>, J. Cox<sup>18</sup>, S.  
Dababneh<sup>8</sup>, G. Daems<sup>9</sup>, M. Dahlfors<sup>9</sup>, V. Dangendorf<sup>19</sup>, S. David<sup>5</sup>, T. Dobers<sup>9</sup>, R. Dolfini<sup>20</sup>, C.  
Domingo-Pardo<sup>21</sup>, I. Duran-Escribano<sup>3</sup>, L. Durieu<sup>9</sup>, C. Eleftheriadis<sup>4</sup>, M. Embid-Segura<sup>12</sup>, A.  
Ferrari<sup>9</sup>, L. Ferreira-Lorenco<sup>22</sup>, R. Ferreira-Marques<sup>15</sup>, C. Flament<sup>9</sup>, H. Fraiss-Koelbl<sup>23</sup>, W. I.  
Furman<sup>24</sup>, M. Gaidon<sup>9</sup>, J. Gascon<sup>9</sup>, D. Gasser<sup>9</sup>, Y. Giomataris<sup>2</sup>, M. Giovannozzi<sup>9</sup>, I. F.  
Goncalves<sup>22</sup>, E. González<sup>12</sup>, I. Goulas<sup>9</sup>, A. Goverdovski<sup>25</sup>, F. Gramegna<sup>10</sup>, E. Griesmayer<sup>23</sup>, F.  
Gunsing<sup>2</sup>, R. Haight<sup>26</sup>, M. Heil<sup>8</sup>, A. Herrera-Martinez<sup>9</sup>, K.G. Ioannides<sup>4</sup>, N. Janeva<sup>27</sup>, E. Jericha<sup>6</sup>,  
Y. Kadi<sup>9</sup>, F. Käppeler<sup>8</sup>, D. Karamanis<sup>4</sup>, M. Kerveno<sup>28</sup>, V. Ketlerov<sup>25</sup>, G. Kitis<sup>4</sup>, P.E. Koehler<sup>29</sup>, V.  
Kononov<sup>24</sup>, E. Kossionides<sup>4</sup>, G. Kowalik<sup>9</sup>, J. Kuhn-Kinell<sup>9</sup>, V. Lacoste<sup>9</sup>, J. M. Lacroix<sup>9</sup>, H.  
Leeb<sup>6</sup>, A. Lindote<sup>15</sup>, I.M. Lopes<sup>15</sup>, M. Lozano<sup>13</sup>, S. Lukic<sup>5</sup>, R. Magnin<sup>9</sup>, E. Mahner<sup>9</sup>, F. Marie<sup>2</sup>, S.  
Markov<sup>27</sup>, S. Marrone<sup>17</sup>, J.M. Martinez-Val<sup>30</sup>, P. Mastinu<sup>10</sup>, A. Mengoni<sup>9</sup>, R. Messerli<sup>9</sup>, G. Metral<sup>9</sup>,  
P. Milazzo<sup>1</sup>, E. Minguez<sup>30</sup>, A. Molina-Coballes<sup>13</sup>, J. Monteiro<sup>9</sup>, C. Moeau<sup>1</sup>, F. Neves<sup>15</sup>, B.  
Nicquevert<sup>9</sup>, R. Nolte<sup>19</sup>, H. Oberhammer<sup>6</sup>, S. O'Brien<sup>18</sup>, J. Pancin<sup>2</sup>, C. Paradela-Dobarro<sup>3</sup>, A.  
Pavlik<sup>31</sup>, P. Pavlopoulos<sup>32</sup>, A. Perez-Parra<sup>12</sup>, J.M. Perlado<sup>30</sup>, L. Perrot<sup>2</sup>, V. Peskov<sup>14</sup>, R. Plag<sup>8</sup>,  
A. Plompen<sup>33</sup>, A. Plukis<sup>2</sup>, A. Poch<sup>11</sup>, M. Poehler<sup>9</sup>, A. Policarpo<sup>15</sup>, C. Pretel<sup>11</sup>, J.M. Quesada<sup>13</sup>, E.  
Radermacher<sup>9</sup>, U. Raich<sup>9</sup>, S. Raman<sup>29</sup>, W. Rapp<sup>8</sup>, T. Rauscher<sup>32</sup>, R. Reifarh<sup>26</sup>, F. Rejmund<sup>5</sup>, J. P.  
Riunaud<sup>9</sup>, G. Rollinger<sup>9</sup>, M. Rosetti<sup>16</sup>, C. Rubbia<sup>20</sup>, G. Rudolf<sup>28</sup>, P. Rullhusen<sup>33</sup>, F. Saldana<sup>9</sup>, J.

<sup>1</sup>Istituto Nazionale di Fisica Nucleare, INFN, Trieste, Italy

<sup>2</sup>Commissariat a l'Energie Atomique (CEA), France

<sup>3</sup>Universidad de Santiago de Compostela, Spain

<sup>4</sup>Astro-Particle Consortium (APC), Greece

<sup>5</sup>Centre National de la Recherche Scientifique/IN2P3 - IPN, Orsay, France

<sup>6</sup>Atominstiüt der Österreichischen Universitäten, Technische Universität Wien, Austria

<sup>7</sup>Charles University, Prague, Czech Republic

<sup>8</sup>Forschungszentrum Karlsruhe, Instiüt für Kernphysik (FZK), Germany

<sup>9</sup>CERN, Geneva, Switzerland

<sup>10</sup>Istituto Nazionale di Fisica Nucleare, INFN, Laboratori Nazionali di Legnaro, Italy

<sup>11</sup>Universidad Politecnica de Catalunya, Barcelona, Spain

<sup>12</sup>Centro de Investigaciones Energeticas Medioambientales y Technologicas (CIEMAT), Madrid, Spain

<sup>13</sup>Universidad de Sevilla, Spain

<sup>14</sup>Kungliga Tekniska Hogskolan, Physics Department (KTH), Stockholm, Sweden

<sup>15</sup>Laboratorio de Instrumentacao e Phisica Experimental de Particulas (LIP),

and Departamento de Fisica da Universidade de Coimbra, Portugal

<sup>16</sup>ENEA, Bologna, Italy

<sup>17</sup>Istituto Nazionale di Fisica Nucleare, INFN, Bari, Italy

<sup>18</sup>University of Notre Dame, USA

<sup>19</sup>Physikalisch Technische Bundesanstalt, Braunschweig, Germany

<sup>20</sup>Università di Pavia, Italy

<sup>21</sup>Consejo Superior de Investigaciones Científicas (CSIC), Universidad de Valencia, Spain

<sup>22</sup>Instituto Tecnológico e Nuclear (ITN), Lisbon, Portugal

<sup>23</sup>Fachhochschule Wiener Neustadt, Wiener Neustadt, Austria

<sup>24</sup>Joint Institute for Nuclear Research, Frank Laboratory of Neutron Physics, Dubna, Russia

<sup>25</sup>Institute of Physics and Power Engineering, Kaluga region, Obninsk, Russia

<sup>26</sup>Los Alamos National Laboratory, New Mexico, USA

<sup>27</sup>Institute for Nuclear Research and Nuclear Energy, Sofia, Bulgaria

<sup>28</sup>Centre National de la Recherche Scientifique/IN2P3 – IReS Strasbourg, France

<sup>29</sup>Oak Ridge National Laboratory, Physics Division, Oak Ridge, USA

<sup>30</sup>Universidad Politecnica de Madrid, Spain

<sup>31</sup>Institut für Isotopenforschung und Kernphysik, Universität Wien, Austria

<sup>32</sup>Department of Physics and Astronomy - University of Basel, Basel, Switzerland

<sup>33</sup>CEC-JRC-IRMM, Geel, Belgium

Salgado<sup>22</sup>, E. Savvidis<sup>4</sup>, M. Silari<sup>9</sup>, J.C. Soares<sup>22</sup>, C. Stephan<sup>5</sup>, G. Tagliente<sup>17</sup>, J.L. Tain<sup>21</sup>, C. Tapia<sup>11</sup>, L. Tassan-Got<sup>5</sup>, L.M.N. Tavora<sup>22</sup>, R. Terlizzi<sup>17</sup>, M. Terrani<sup>20</sup>, N. Tsangas<sup>4</sup>, W. Van Baaren<sup>9</sup>, G. Vannini<sup>1</sup>, P. Vaz<sup>22</sup>, A. Ventura<sup>16</sup>, D. Villamarin-Fernandez<sup>12</sup>, M. Vincente-Vincente<sup>12</sup>, V. Vlachoudis<sup>9</sup>, R. Vlastou<sup>4</sup>, F. Voss<sup>8</sup>, M. Weierganz<sup>19</sup>, H. Wendler<sup>9</sup>, M. Wiescher<sup>18</sup>, K. Wisshak<sup>8</sup>, L. Zanini<sup>9</sup>, M. Zanolli<sup>9</sup>.

---

<sup>1</sup>Dipartimento di Fisica and INFN, Bologna, Italy

## 1 Premise

This proposal represents a continuation of the measurement campaign undertaken by the n\_TOF collaboration on fission cross sections relevant to advanced nuclear fuel cycles and incineration of nuclear waste. The proposal for the measurement of fission cross sections induced by neutrons on isotopes relevant to the thorium fuel cycle (INTC/P-145 and INTC/P-145-Addendum) has been presented and approved in 2002 (experiment n\_TOF-06). The measurement of some of the isotopes involved in that proposal has been performed during the n\_TOF 2002 measurement campaign.

Here we propose the measurement of fission cross sections of minor actinides, specifically of  $^{237}\text{Np}$ ,  $^{241,243}\text{Am}$ , and  $^{245}\text{Cm}$ . Some of the isotopes included in n\_TOF-06 (for example  $^{234}\text{U}$  and  $^{236}\text{U}$ ) will be part of the 2003 measurement campaign as well. They are therefore included in part of the discussion of the present proposal.

## 2 Motivations

Trans-Uranium elements (TRU) such as Np, Pu, Am and Cm are built up as a result of multiple neutron captures and radioactive decays in the presently operating nuclear reactors based on the U/Pu nuclear fuel cycle. Some highly active isotopes of these elements constitute the most important hazard for nuclear waste management. Recently, several proposals have been made to reduce the radiotoxicity of nuclear waste containing TRU. They all rely on neutron induced capture and fission of the TRU, in particular of  $^{237}\text{Np}$ ,  $^{241,243}\text{Am}$ , and  $^{244,245}\text{Cm}$ . It is clear that any kind of waste burner system, critical or sub-critical, thermal or fast, will need to be loaded with fuel containing a large fraction of TRU. The response of these systems (e.g. criticality conditions) to the presence of TRU is directly linked to the fission and capture cross sections of the mentioned TRU isotopes. The fission cross sections of TRU are therefore fundamental elements in assessing the strategy to be followed in detailed feasibility studies of nuclear waste transmutation.

A peculiarity of the fission process in the higher actinides in consideration here (with the exception of  $^{245}\text{Cm}$ ) is that they have a relatively high fission threshold, above a few hundred keV. This is one of the considerations which led to the proposal for accelerator driven systems (ADS) [1], in which a fast neutron spectrum is considered for transmutation. The situation is clearly shown in Figure 1. There, the neutron spectrum of an ADS based on a Pb-Bi cooled reactor [2], loaded with a fuel mixture of minor actinides (Spiro MA mixture) is shown together with the fission cross sections of several TRU isotopes. The fission cross section of  $^{239}\text{Pu}$  is also shown for a direct comparison with a case in which no threshold is present.

In addition, in some advanced fuel cycle scenarios the contribution of  $^{237}\text{Np}$  and  $^{241}\text{Am}$  to the total fission rate can be as large as 10% [3] and the fraction of sub-threshold fission typically of 5% even in a fast spectrum. Therefore, both below and above threshold these isotopes represent important contributions to the global reactor neutron balance. In the case of  $^{245}\text{Cm}$ , fission represents nearly 90% of the neutron absorption in fast neutron spectra, and its contribution to the global fission rate is expected to be larger than 6% in some ADS fuelled with MA. Direct fission is the most important channel for the transmutation of this isotope. Furthermore, the fission

cross sections of the isotopes in consideration here play an important role on the precise definition of the isotopic content of the transmutation ADS discharged fuel.

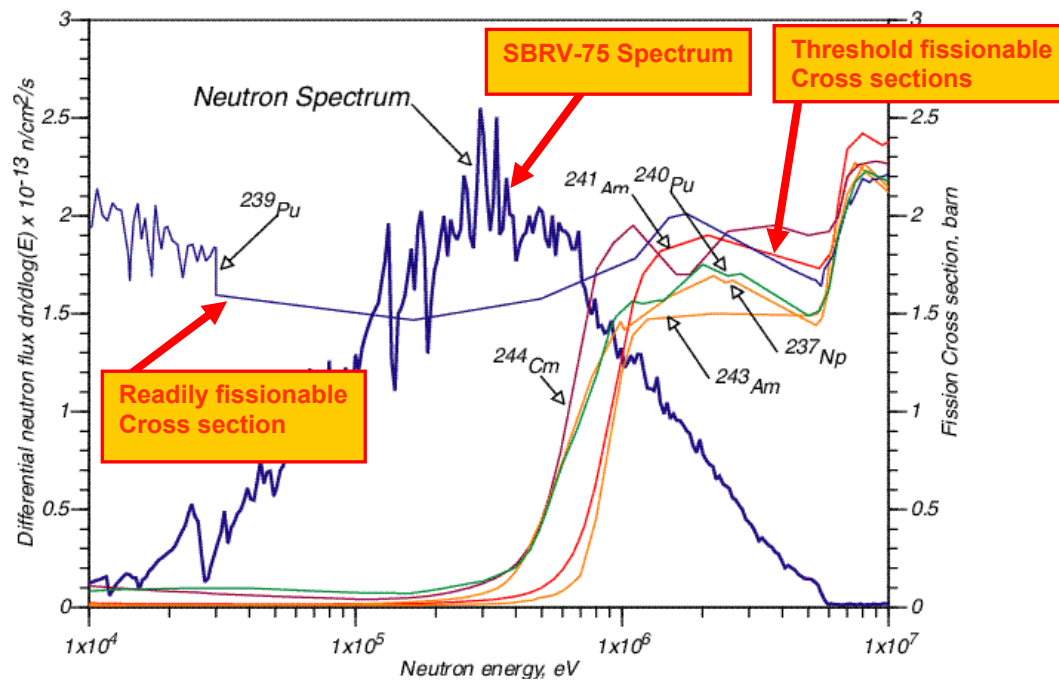


Figure 1: Simulation of the neutron spectrum in the SBRV-75 reactor [2], loaded with the Spiro MA fuel mixture (1/2 of  $^{241}\text{Am}$ , 1/4 of  $^{243}\text{Am}$  and 1/4 of equal amount of  $^{244}\text{Cm}$  and  $^{237}\text{Np}$ ). The fission cross sections of several MA in consideration here are shown. The fission cross section of  $^{239}\text{Pu}$  is also shown for a direct comparison with a non-threshold fission case.

From these considerations it appears that for the design and operation of such a class of advanced systems it is necessary to have access to nuclear data bases which include accurate fission cross sections in a much wider range as compared to those in use for thermal systems, for neutron energies up to at least several MeV.

The presence of the fission threshold and of the sub-threshold resonance structure in some of the higher actinides allow for studies of the outer fission barrier, as well as of the structure (hyper-deformation) of the fission potential. The very high resolution of the n\_TOF beam provides a unique opportunity to address some of the open questions concerning the structure of sub-threshold vibrational resonances as already shown in the  $^{234}\text{U}(n,f)$  measurement performed in 2002.

With these basic motivations, the n\_TOF Collaboration has proposed to perform neutron induced fission cross section measurements using the CERN n\_TOF facility. The neutron beam characteristics and experimental conditions at n\_TOF are optimal for measurements of fission cross sections on radioactive materials [4]. This is mostly due to the extremely high instantaneous flux obtained from the spallation process driven by the 20 GeV proton beam from the CERN-PS. The high proton beam intensity ( $7 \times 10^{12}$  protons/pulse), the  $1.2 \text{ s}^{-1}$  pulse frequency and the long flight-path (approximately 185 m), represent optimal conditions for high resolution cross section measurements. As will be shown in detail below, the unsatisfactory situation of

nuclear data in the presently available libraries could be substantially improved by the present proposal for measurements at n\_TOF.

The preliminary results obtained during the 2002 measurement campaign on isotopes relevant for the Thorium fuel cycle, notably  $^{232}\text{Th}$  and  $^{234}\text{U}$ , provide the necessary confidence in the operation of the fission detectors and on the achievable accuracy in the energy range  $1 \text{ eV} \leq E_n \leq 250 \text{ MeV}$ .

Combining the basic motivations with the availability of target materials, we propose a measurement of the fission cross sections of  $^{237}\text{Np}$ ,  $^{241,243}\text{Am}$ , and  $^{245}\text{Cm}$ .

### 3 Status of nuclear data on fission cross section of minor actinides

A brief description of the present situation of nuclear data on fission cross section of the nuclei relevant for the present proposal is given here below. The set of figures referred to here are given in the Appendix. The data shown in the figures are those presently available in the EXFOR data file [5]. In the description, however, we have also considered data from additional measurements which are not present in the EXFOR compilation.

**Neptunium-237.** Several measurements of the fission cross section of  $^{237}\text{Np}$  have been made previously, below and above threshold. However, the quality of the data is not always acceptable, in accuracy as well as concerning the energy range covered. In particular, in the sub-threshold resonance energy region,  $^{237}\text{Np}$  has a small fission cross section which is important for transmutation studies in Pb or Pb-Bi cooled systems, where the epithermal neutron flux is not negligible in the periphery of the fuel core, and where some proposal to perform heterogeneous transmutation of minor actinides has been made. Recent measurements by Yamanaka *et al.* [6] carried out at the Kyoto University Lead Slowing-down Spectrometer (KULS) and used in JENDL-3.2 are a factor of three higher than those measured by Plattard *et al.* [7] on which the ENDF/B-VI evaluated file is based. This is so, consistently, over the energy range between 1 eV and 0.5 keV (see Figure A-1), even after correcting for the poor energy resolution ( $\Delta E/E = 40\%$ ) the KULS data. The latest measurements of Carlson *et al.* [8] has confirmed this discrepancy. Above 1 MeV the latest work suggests, however, a rather good agreement with the ENDF/B-VI evaluation which in this energy range is about 5% lower (see Figure A-2). The wide neutron energy range covered by the n\_TOF beam would allow for a more consistent and accurate definition of the threshold and of the upper energy range. In the sub-threshold region, in particular in the energy range up to 10 eV, a more accurate determination of resonance parameters can also be expected (see Figure A-1).

**Americium-241:** Measurements of the fission cross section of  $^{241}\text{Am}$  are difficult to perform because of the extremely high  $\alpha$ -particle activity of this nuclide. Its half-life against  $\alpha$ -decay is 433 yr. Given the characteristics of the n\_TOF neutron beam, in particular its high instantaneous flux, a measurement at n\_TOF can improve the signal/noise ratio by a large factor. In addition to these difficulties, the fission

cross section of  $^{241}\text{Am}$  is lower than 0.5 b over the range between 1 keV to 300 keV. Several measurements exist in the threshold region [9,10,11,12,13,14,15,16,17], but the most recent [15-17] differ amongst each other by more than 14%, below the threshold. The evaluated data files JENDL-3 and ENDF/B-VI, which mainly refer to the experimental data by Dabbs *et al.* [14], are in disagreement with the earlier data by Bowman *et al.* [9], Seeger *et al.* [10], Gayther *et al.* [13], and Knitter *et al.* [15], in the energy region above about 30 eV. The latest measurements of Kobayashi *et al.* [18] are a factor of three higher than the evaluated data, even after correcting for the poor energy resolution of 40% (see Figure A-3). These results were also compared with the existing experimental data in Figure A-4, which show that the data by Dabbs *et al.* [14] are about 3 times smaller. Those by Seeger *et al.* [10] are much larger above 100 keV, but the data by Knitter *et al.* [15] are much smaller. The fission cross sections by Gayther *et al.* [13] and Bowman *et al.* [9] are rather close to these new measurements in the relevant energy range. The data measured in the MeV energy region show however good agreement with each other (Figure A-5). In conclusion, given the present situation of the available nuclear data, we can expect that the energy resolution of n\_TOF would allow to explore the detailed structure of the  $^{241}\text{Am}(n,f)$  cross section, below and above the fast fission threshold.

**Americium-243:** In the case of  $^{243}\text{Am}$ , there exist a very limited number of experimental data in the EXFOR data base in the lower energy region [19,20,21]. Seeger *et al.* [19] measured the fission cross section above 50 eV using a nuclear explosion experiment, and Wisshak *et al.* [20] determined the neutron capture and fission cross sections in the energy range from 5 to 250 keV with a Van de Graaff accelerator. Knitter *et al.* [21] measured the resonance parameters between 1 and 100 eV and the fission cross sections above 100 eV with an electron linear accelerator. The comparison between the latest measurements by Kobayashi *et al.* [22] with the evaluated cross sections in ENDF/B-VI and JENDL-3.2 shows some discrepancies between both evaluated data in the energy regions below 0.3 eV and above 15 eV. Although the ENDF/B-VI data are in agreement with the measurements, they are lower at energies between 15 and 60 eV. The JENDL-3.2 data seem to be lower than the measurements above 100 eV. When comparing the latest measurements with existing experimental data (Figure A-6), it appears that the data by Wisshak *et al.* [20] and Knitter *et al.* [21] are in agreement, however, the results by Seeger *et al.* [19] are considerably higher above several hundred eV. The data measured in the MeV energy region show good agreement amongst each other (Figure A-7). Again, as in the case of  $^{241}\text{Am}$ , the energy resolution of n\_TOF would allow to explore the detailed structure of the cross section, in the fission threshold region as well as above. An improved determination of the resonance parameters in the very low energy region can also be attempted in this case.

**Curium-245.** In the case of  $^{245}\text{Cm}$ , there are very few experimental data available in the lower energy region [23,24,25,26,27]. Ivanin *et al.* [26] determined the fission cross section in the energy range from 100 keV to 10 MeV with the white neutron source of the VNIIEF 50 MeV electron linac, a measurement based on the time-of-flight technique. Gerasimov *et al.* [27] measured the fission cross sections below 40 keV using the lead slowing-down spectrometer driven by the high current

electron linac “Fakel” at Kurchatov Institute. The evaluated data for this isotope are generally in poor agreement with the measurements (Figure A-8). In the energy region around and above 1 MeV, a comparison amongst different measurements show poor agreement (Figure A-9), with the evaluated data generally scattered over a wide range. It is expected that the proposed measurement would allow for an accurate determination of the resonance parameters in the low energy region and a substantial improvement of the situation above 1 MeV.

## 4 Experimental setup

The proposed measurements of fission cross sections will be performed with two separate detection systems. One based on parallel plate avalanche counters (PPAC), and a Fast Ionization Chamber (FIC). A detailed description of the principles of operation of both detection systems is given in reference [4] (see pages 89-95). Here we will limit ourselves to describe the specific setup of the two detection systems for the measurement in consideration. A schematic view of the setup is given in Figure 2.

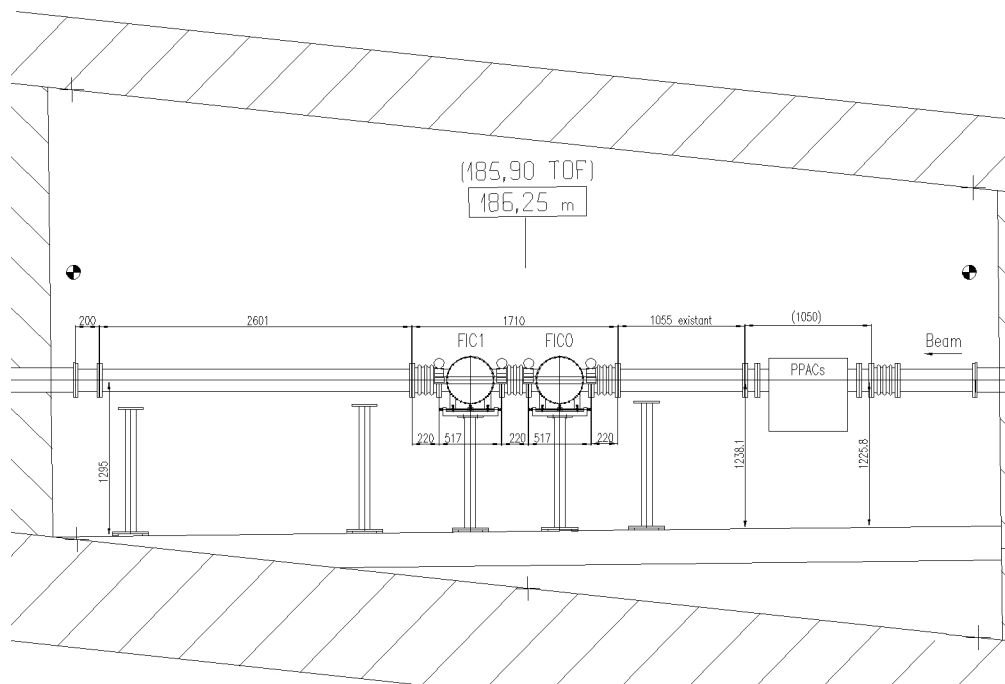


Figure 2: schematic view of the fission setup configuration of the n\_TOF experimental area.

A general point can be briefly mentioned here concerning the motivation for using the proposed setup. The two detection systems are based on completely different principles, in particular with respect to  $\alpha$  pile-up and self-absorption effects. Therefore they are subject to different and independent systematic uncertainties. This will allow us to derive a more consistent set of cross section data.



#### 4.1 The Parallel Plate Avalanche Detector (PPAC)

The detector chamber will contain targets used as standard ( $^{235}\text{U}$  and  $^{238}\text{U}$ ) as well as the targets of the material to be studied in the present experiment. Both standard samples are of very high purity, the  $^{235}\text{U}$  containing only 0.3% of  $^{234}\text{U}$  and 0.3% of  $^{236}\text{U}$ , while the  $^{238}\text{U}$  sample is practically free of contaminations since it was produced by means of the isotope separator SIDONIE. These targets are prepared at Orsay by electro-deposition on pure, 2  $\mu\text{m}$  thick aluminium backings. They will serve for normalization of the relative fission cross sections and as flux monitors.

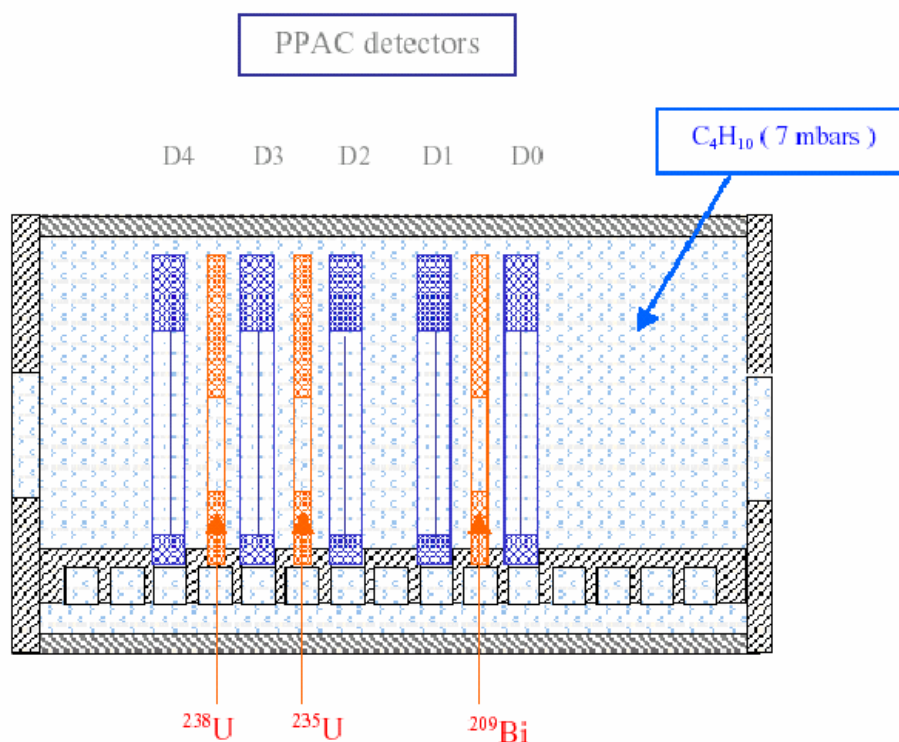


Figure 3: A schematic view of the PPACs detector.

The actinide targets (see Table 1 for the complete list of isotopes) are also deposited on 2  $\mu\text{m}$  aluminium foils, which are thin enough to allow the coincident detection of the fission fragments<sup>1</sup>.

<sup>1</sup>The behaviour of these backings under heavy  $\alpha$  irradiation (typically  $8 \times 10^{14}$   $\alpha/\text{cm}^2$  per year for the suggested  $^{241}\text{Am}$  sample) can be estimated as follows: the total energy deposited in the backing in one year is comparable to the energy deposited in a target of the same thickness irradiated at GANIL during about one day with a 40 MeV/nucleon argon beam of 100 nA. Such a target can afford a week irradiation by this beam intensity without damage. Given the time span in which the targets will be prepared and measured (a few months), we can expect no major damage of the thin backings due to the sample  $\alpha$  activity.

On both sides of each target two 20×20 cm<sup>2</sup> PPACs are used for detecting the fission fragments and to measure their position of origin. The PPACs and the respective targets are separated by a gap of 5 mm. As the PPACs operate at very low gas pressure (7 mbar), the target and the PPACs will be placed inside a vacuum chamber. A total of 9 targets including those used as flux monitors and standards will be measured simultaneously.

The solid angle covered by a PPAC pair is almost  $4\pi$ , but the effective solid angle is reduced due to self-absorption in the sample, in the backing, and in the entrance electrode of the PPACs. From simulations and from the previous measurements performed with the present setup, we conclude that 300  $\mu\text{g}/\text{cm}^2$  thick samples constitute an optimal compromise. As a result, the actual solid angle and, hence, the detection efficiency for fission fragments is limited to 50%.

Table 1: Description of the different setups for fission cross section measurements with PPACs (isotope, sample diameter, mass, and activity) The total amount of  $\alpha$  radioactivity as well as the number of protons required for each setup is given.

										Total activity	Number of protons
										[Bq]	[10 <sup>18</sup> ]
<b>Setup 1</b>											
Target	<sup>238</sup> U	<sup>235</sup> U	<sup>232</sup> Th	<sup>232</sup> Th	<sup>232</sup> Th	<sup>232</sup> Th	<sup>232</sup> Th	<sup>234</sup> U	<sup>234</sup> U	6×10 <sup>6</sup>	2
∅ [cm]	8	8	8	8	8	8	8	8	8		
mass [ $\mu\text{g}/\text{cm}^2$ ]	300	300	300	300	300	300	300	300	300		
activity [Bq]	185	1200	44	44	44	44	44	3×10 <sup>6</sup>	3×10 <sup>6</sup>		
<b>Setup 2</b>											
Target	<sup>238</sup> U	<sup>235</sup> U	<sup>233</sup> U	<sup>233</sup> U	<sup>237</sup> Np	<sup>237</sup> Np	<sup>237</sup> Np	<sup>237</sup> Np	<sup>237</sup> Np	1.1×10 <sup>7</sup>	0.5
∅ [cm]	8	8	8	8	8	8	8	8	8		
mass [ $\mu\text{g}/\text{cm}^2$ ]	300	300	300	300	300	300	300	300	300		
activity [Bq]	185	1200	5×10 <sup>6</sup>	5×10 <sup>6</sup>	3×10 <sup>5</sup>	3×10 <sup>5</sup>	3×10 <sup>5</sup>	3×10 <sup>5</sup>	3×10 <sup>5</sup>		
<b>Setup 3</b>											
Target	<sup>238</sup> U	<sup>235</sup> U	<sup>236</sup> U	<sup>236</sup> U	<sup>236</sup> U	<sup>236</sup> U	<sup>237</sup> Np	<sup>237</sup> Np	<sup>237</sup> Np	1.0×10 <sup>6</sup>	1.5
∅ [cm]	8	8	8	8	8	8	8	8	8		
mass [ $\mu\text{g}/\text{cm}^2$ ]	300	300	300	300	300	300	300	300	300		
activity [Bq]	185	1200	3×10 <sup>4</sup>	3×10 <sup>4</sup>	3×10 <sup>4</sup>	3×10 <sup>4</sup>	3×10 <sup>5</sup>	3×10 <sup>5</sup>	3×10 <sup>5</sup>		
<b>Setup 4</b>											
Target	<sup>238</sup> U	<sup>235</sup> U	<sup>243</sup> Am		<sup>243</sup> Am		<sup>243</sup> Am		<sup>243</sup> Am	2.0×10 <sup>8</sup>	1
∅ [cm]	8	8	6		6		6		6		
mass [ $\mu\text{g}/\text{cm}^2$ ]	300	300	140		140		140		140		
activity [Bq]	185	1200	5×10 <sup>7</sup>		5×10 <sup>7</sup>		5×10 <sup>7</sup>		5×10 <sup>7</sup>		
<b>Setup 5</b>											
Target	<sup>238</sup> U	<sup>235</sup> U	<sup>241</sup> Am		<sup>241</sup> Am		<sup>241</sup> Am		<sup>241</sup> Am	2.0×10 <sup>8</sup>	10
∅ [cm]	8	8	2		2		2		2		
mass [ $\mu\text{g}/\text{cm}^2$ ]	300	300	130		130		130		130		
activity [Bq]	185	1200	5×10 <sup>7</sup>		5×10 <sup>7</sup>		5×10 <sup>7</sup>		5×10 <sup>7</sup>		

With the PPACs also very good spatial resolution can be achieved. The detector foils on each side of the anode are divided into 2 mm wide strips, and the anode itself is made of a similar double-sided, aluminium-plated Mylar foil. The position sensitivity allows us to measure the neutron flux at each point on the target. Therefore, having a map of the flux for each neutron energy bin, variations of the beam shape with energy, the non-uniformity of the sample, and the effective sample size can be accounted for. Being the thinnest available detectors for timing and position sensitive measurements, PPACs are practically transparent to neutrons and  $\gamma$ -rays and insensitive to radiation damage.

The PPAC anodes are connected to current preamplifiers delivering signals of 15 ns total width, with less than 1 ns time resolution. This anode signal enters a 1GHz Flash ADC of 8 bit resolution and provides the neutron arrival time. The strips of the cathodes are connected to delay lines with each delay cell inducing a 3 ns delay, allowing thus a position determination from the delayed signals collected at both ends of the delay line. These signals are also processed by a 1GHz Flash ADC of 8 bit pulse height resolution. The pulse height information and the detection of the two fission fragments in coincidence provide an efficient discrimination between fission fragments and alpha particles.

Due the excellent timing of the detectors, the neutron energy resolution is not affected by the experimental set-up, but is completely defined by the n\_TOF facility, i.e. by the pulse width of the proton beam (7 ns) and the moderation time.

## 4.2 *The Fast Ionization Chamber (FIC)*

Two Fast Ionization Chambers, FIC-0 and FIC-1, will be used in the 2003 runs. FIC-0, the counter used in the 2002 campaign, will be essentially dedicated to the measurement of samples with relatively low activity ( $^{234,236}\text{U}$  and  $^{237}\text{Np}$ ), whereas FIC-1 will be used for highly radioactive samples ( $^{233}\text{U}$ ,  $^{241,243}\text{Am}$  and  $^{245}\text{Cm}$ ). The two chambers are foreseen to be mounted as schematically shown in Figure 2.

Following the good results achieved in the 2002 for  $^{234}\text{U}$  [4], a new detector based on the same principle [28] has been designed for the measurement of highly radioactive isotopes like Am and Cm. This new version of the detector, FIC-1, will be qualified as “sealed source” according with the international standard ISO 2919. Since the ionization chamber is not working in proportional mode, a gas flow can be avoided thus facilitating the design of a “sealed” detector body.

A comparison between the simulations [29] and the data taken with FIC-0 in 2002 is reported in Figure 5. The fission fragment events are recognized by simple amplitude discrimination with efficiency very close to 100%, limited only by the fission fragments absorption in the target itself. With a deposit density of  $\sim 150 \mu\text{g}/\text{cm}^2$  the measured efficiency in FIC-0 is 95%.

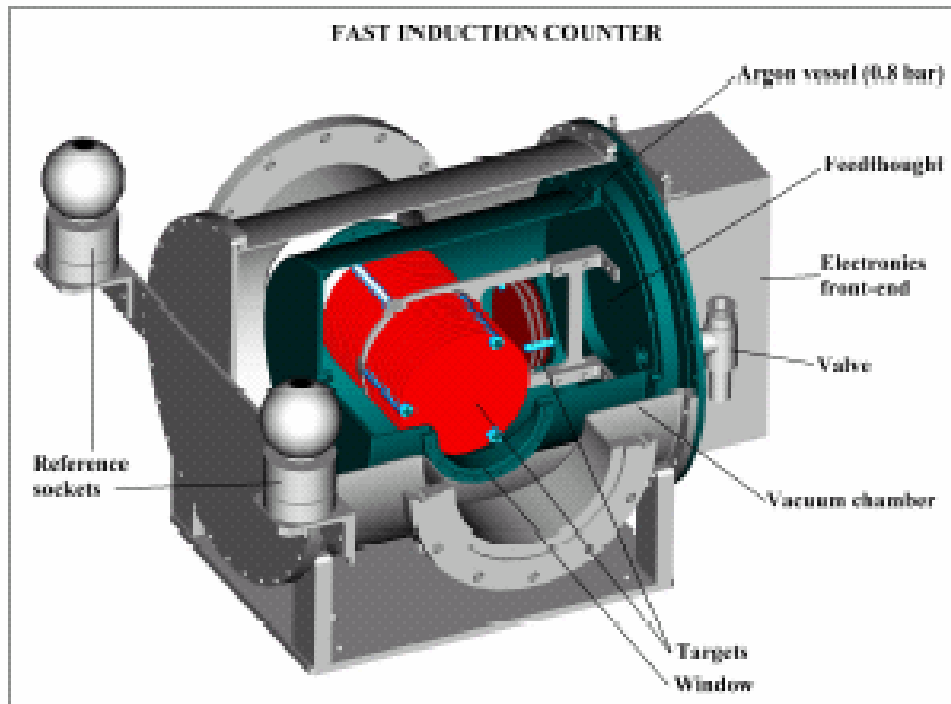


Figure 4: a schematic view of the FIC detector

Among the isotopes foreseen for fission measurements in 2003, there are several cases in which the alpha background is at a level that may constitute a problem in the measurements. In order to estimate this effect, we have performed a full simulation of the worst case, that of  $^{241}\text{Am}$ , which has a half-life of 433 yr and an alpha activity over  $4\pi$  of  $1.27 \times 10^8$  Bq/mg. This level of activity induces pile up of signals, increasing the difficulty in the discrimination of the fission events. The energy of the most intense  $\alpha$ 's (85% of the total) is 5.49 MeV and the other important decays are of lower energy. We consider a maximum mass of the sample of  $^{241}\text{Am}$  of 0.5 mg, corresponding to 0.565 mg of  $\text{AmO}_2$  sample with a density of  $11.68 \text{ g/cm}^3$  (equivalent to one of the four targets included in the list of Table 3).

The simulations for  $^{241}\text{Am}$ , assuming FIC-1 working in the same conditions of FIC-0, are reported in Figure 6. The nominal working conditions for the FIC detectors are:

- Gas pressure: 720 mbar (90% Ar – 10%  $\text{CF}_4$ )
- Electric field: 600 V/cm
- Electron drift velocity: 120 mm/ $\mu\text{s}$
- Gap between electrodes: 5 mm

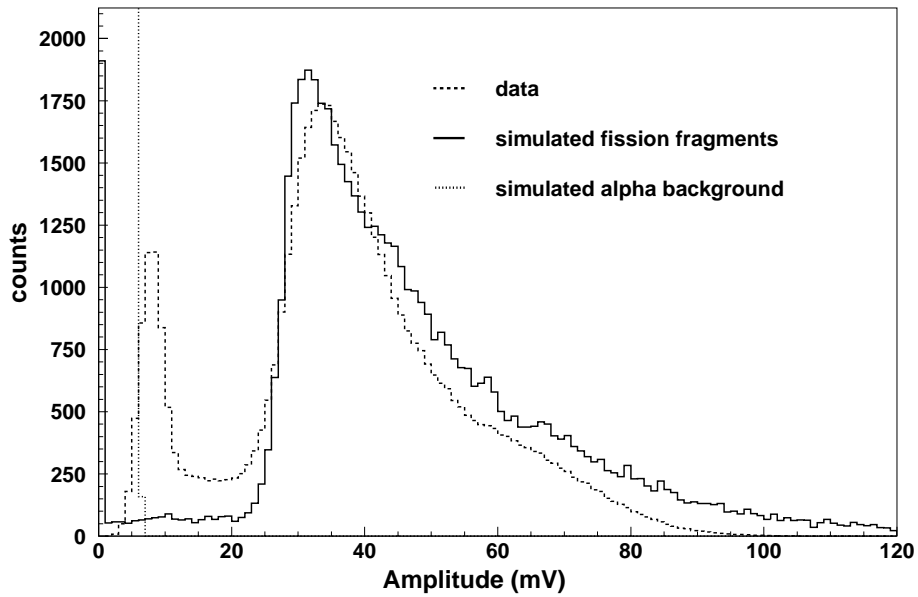


Figure 5: Comparison between simulation and the  $^{235}\text{U}$  data taken with FIC-0 in the 2002 run. The simulated signal from the alpha particles is represented by the almost vertical line, in the low amplitude region. The peak in the 8 mV region in the measured data is the result of electronic noise and is therefore not related to the signal from alphas.

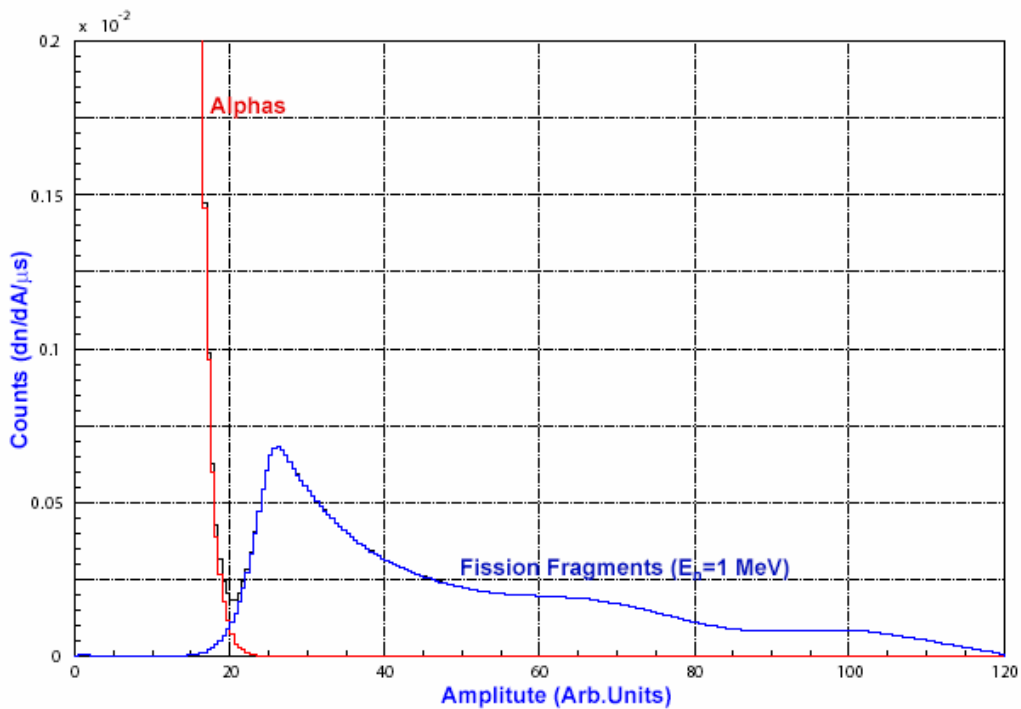


Figure 6: Simulation of FIC-1 under nominal working conditions. The signal produced by the alpha activity for 0.5 mg of  $^{241}\text{Am}$  (including pile-ups) is shown together with the amplitude distribution of the fragments emitted following fission. The time window for both types of signal is 1  $\mu\text{s}$ , around tof corresponding to 1 MeV neutrons. Even though the rate due to the  $\alpha$  activity is very large, the signal from the fission fragments is still clearly separable.

It is clear that due to the high activity of the  $^{241}\text{Am}$  sample and consequently of the expected pile-ups, the situation is much more difficult as compared with that represented in Figure 5. However, even in this case (the worse of all the presently considered samples), by applying a discrimination threshold there will be the possibility of a clear separation between alpha background and fission fragments signatures.

The basic information on the targets which will be mounted respectively in the detector FIC-0 and FIC-1 are reported in Table 2 and Table 3, respectively

Of the isotopes listed in the tables, those related to the present proposal are  $^{237}\text{Np}$ ,  $^{241,243}\text{Am}$ , and  $^{245}\text{Cm}$ . In addition to these, one notices for example  $^{234}\text{U}$  which has been already included in 2002 measurement. In fact, the data collected so far for the neutron induced cross-section of  $^{234}\text{U}$  are under analysis to investigate the fine structure of the vibrational resonances associated with quasi-stationary states in the second hyperdeformed potential well of the  $^{235}\text{U}$  compound nucleus. To finalize the measurement, additional statistics are needed for this isotope.

Table 2: List of isotopes mounted in FIC-0.  $^{237}\text{Np}$  is the isotope concerned in the present proposal.

Item	Isotope	$\varnothing$ [mm]	Mass [mg]	Density [ $\mu\text{g}/\text{cm}^2$ ]	Position	Number of targets
1	U-234	50	33.75	~150	Beam	6
2	U-235	50	17	~200	Beam	2
3	U-235	80	30	~300	Beam	1
4	U-235	60	51	~450	Bckg.	2
5	U-238	50	30	~250	Beam	3
6	U-238	80	60	~300	Beam	2
7	U-238	60	34	~300	Bckg.	2
8	U-236	80	20	~100	Beam	2
9	Th-232	80	80	~400	Beam	2
<b>10</b>	<b>Np-237</b>	<b>80</b>	<b>15</b>	<b>~150</b>	<b>Beam</b>	<b>1</b>
11	Dummy				Beam	1

There are, altogether, 19 and 16 targets respectively in FIC-0 and FIC-1 in the beam direction and 4 targets normal to it. This allows the evaluation of the background produced by scattered neutrons on the detector structure. A dummy target is inserted in the neutron beam direction to subtract the signal eventually produced in the chamber at  $t_0$ .

Table 3: List of isotopes mounted in FIC-1. 241,243Am and 245Cm are the isotopes concerned in the present proposal.

Item	Isotope	Ø [mm]	Mass [mg]	Density [ $\mu\text{g}/\text{cm}^2$ ]	Position	Number of targets
1	Am-241	80	2	~5	Beam	4
2	Am-243	80	10	~25	Beam	4
3	Cm-245	80	2	~10	Beam	2
4	U-233	80	20	~100	Beam	2
5	U-235	80	30	~300	Beam	1
6	U-235	60	51	~450	Bckg.	2
7	U-238	80	60	~300	Beam	2
8	U-238	60	34	~300	Bckg.	2
9	Dummy				Beam	1

## 5 Radioprotection and safety aspects

Several radioprotection aspects arise when dealing with the high intrinsic activity of higher actinides. In particular, due to the high activity of the americium and curium isotopes, the Swiss authorities request a high level of safety for the fission detectors. The main obligation is that the detector vessels containing the radioactive samples should be considered as sealed, and should comply with the ISO-2919 norm for sealed radioactive sources. For moderately radioactive samples such as  $^{235}\text{U}$ ,  $^{238}\text{U}$ ,  $^{237}\text{Np}$ , the mounting and dismounting of samples from the vessel can be done in the hot laboratory at CERN, whereas for the americium and curium samples the operation will be done at the class-A hot-laboratory of PSI-Villigen. For the PPAC, the detector chamber will be transported to CERN with the samples already mounted and with the chamber sealed, an operation already performed during the 2002 measuring campaign.

Tables with the level of activity of the samples to be used in the two sets of fission detectors are given in Table 1 for PPACs and here below (Table 4) for the FIC detectors.

Table 4: Radioactivity of the FIC target materials. LA stands for “Legal Authorization” and represents, for each nuclide, the activity threshold above which a substance needs to be treated following radioprotection rules.

Item	Isotope	Specific Activity [Bq/mg]	LA [Bq]	Mass [mg]	Activity [Bq]	LA Index
1	Am-241	$1.27 \times 10^8$	200	2	$2.54 \times 10^8$	$1.27 \times 10^6$
2	Am-243	$7.37 \times 10^6$	200	10	$7.37 \times 10^7$	$3.69 \times 10^5$
3	Cm-245	$6.35 \times 10^6$	200	2	$1.27 \times 10^7$	$6.35 \times 10^4$
4	U-233	$3.57 \times 10^5$	700	20	$7.14 \times 10^6$	$1.02 \times 10^4$
5	U-235	79.96	800	81	$6.48 \times 10^3$	8.1
6	U-238	12.34	900	34	$4.20 \times 10^2$	0.47

A thin lead shielding will be installed around the detectors to keep the radioactivity at the level in agreement with the CERN radioprotection rules. If necessary, the shielding will be provided with removable windows in the direction of the neutron beam to minimize the neutron scattering along the neutron path.

As other practical aspects are different for the PPAC and FIC detectors they will be described separately in the two following sub-sections.

### **5.1 PPAC**

For the PPAC chamber a gas flow is needed to renew the gas in the detection gaps. This means that the chamber can not strictly be considered a sealed source. Therefore, we propose three additional safety measures:

1. The gas will be kept in a closed system. The used counting gas is collected in an evacuated 300 l container, from where the gas will be released once per month under the control of TIS.
2. A filter will be placed behind the circulating pump to trap any radioactive powder or dust.
3. Electromagnetic valves will be placed in the gas pipes immediately at the vessel to ensure tight insulation in case of unexpected events (abnormal changes in pressure, vacuum, and temperature, or electricity failure). This implies that the vessel is sealed even under emergency conditions.

In addition, smoke and temperature detectors will be installed in the vicinity of the chamber to trigger an immediate warning in case of fire. Since the gas pressure is very low (7 mbar), any leak will cause an inward air flow into the detector vessel, thus preventing any dispersion of material outside the detector. The chamber containing the radioactive samples will be shipped to CERN as a sealed container, as it was the case in 2002.

### **5.2 FIC**

The activities expected in FIC-1 are reported in Table 4. The very large LA index ( $1.7 \times 10^6$ ) explains the need to use a special detector body certified as sealed.

For FIC-0 a special authorization has been already given by the Swiss radioprotection authorities. Concerning FIC-1, the detector will be certified as “sealed” according to the ISO 2919 standard.

## **6 Count-rate estimate and number of proton request**

The estimated count rates are based on the quantities given in Table 1 for PPACs, in Table 4 for FIC detectors, and on the efficiencies resulting from the data taken in 2002. The number of fission events expected for the various isotopes is comprised between 250 and 1000 at 1 MeV neutron energy, with 1% energy binning (230 bins/energy-decade) and  $10^{18}$  protons. The rates at this energy are significant, for the isotopes concerned, in the range just above the threshold where the cross sections



of the different isotopes are comparable. In the sub-threshold region, for resonances in the energy region up to 10 eV, a statistical uncertainty of a few percent can be expected for isolated resonances, assuming the same energy binning (1%). This would be sufficient, for example, to solve the discrepancies observed in the sub-threshold resonance parameters, which are up to 50%, in the present situation.

Since the measurement could be done with both detection systems in operation and with all the samples in the FIC chambers mounted at the same time, the measurement of fission cross sections for the present proposal could be made with the required accuracy by using  $5 \times 10^{18}$  protons, in the fission mode configuration (with the Ø8cm collimator). The only exception is the setup-5 for the PPAC detector, where  $10 \times 10^{18}$  protons would be needed. However, in this case the maximum sample diameter would be of 2 cm, therefore the additional  $5 \times 10^{18}$  protons could result from runs in parallel with a capture measurement setup. This configuration has been already tested in the 2001 and 2002 measurement campaigns.

In conclusion, the total request for the present proposal is of  **$5 \times 10^{18}$  protons.**

# **APPENDIX**

# $^{237}\text{Np}(n,f)$

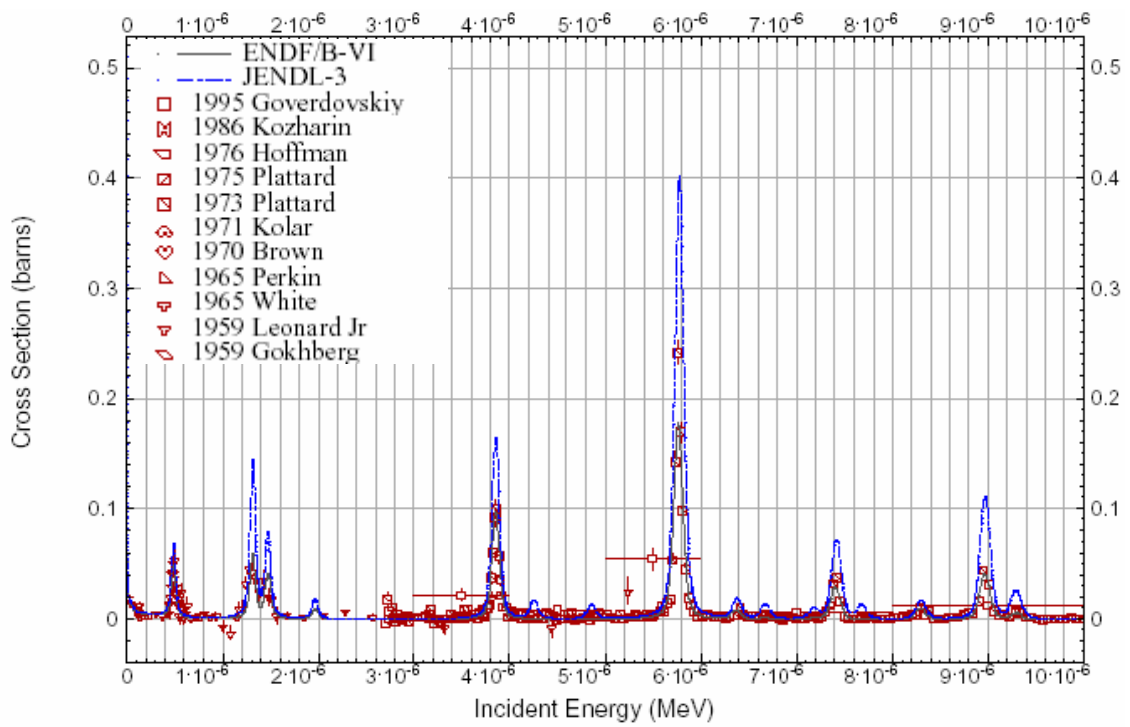


Figure A-1: fission cross section of  $^{237}\text{Np}$  in the low energy region,  $E_n \leq 10$  eV, well below the fission threshold.

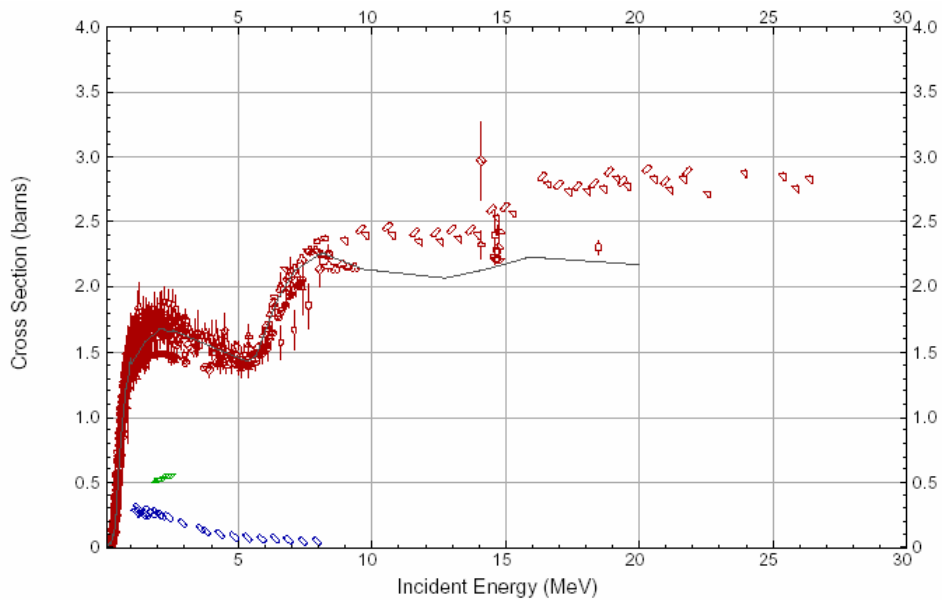


Figure A-2: fission cross section of  $^{237}\text{Np}$  in the high energy region, in and above the fission threshold.

# $^{241}\text{Am}(n,f)$

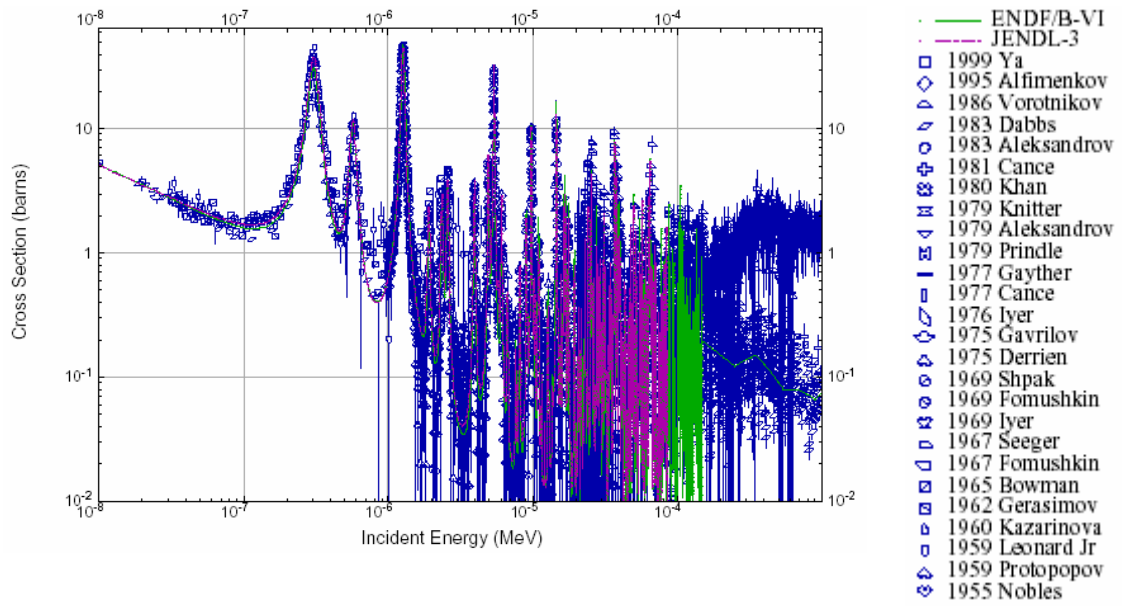


Figure A-3: fission cross section of  $^{241}\text{Am}$  in the low energy region.

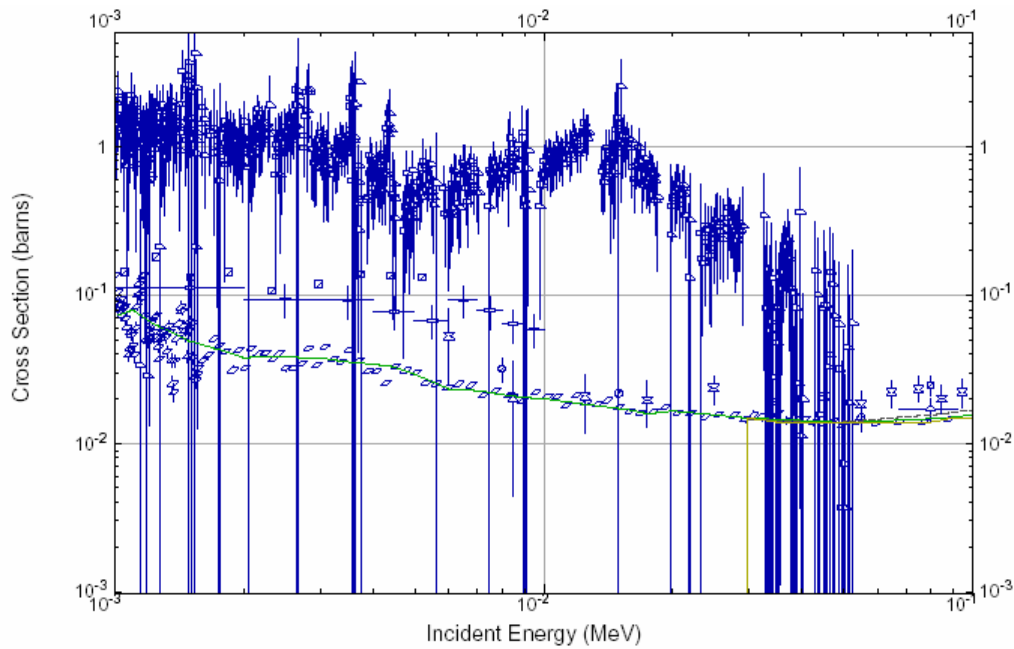


Figure A-4: fission cross section of  $^{241}\text{Am}$  in the low energy part.

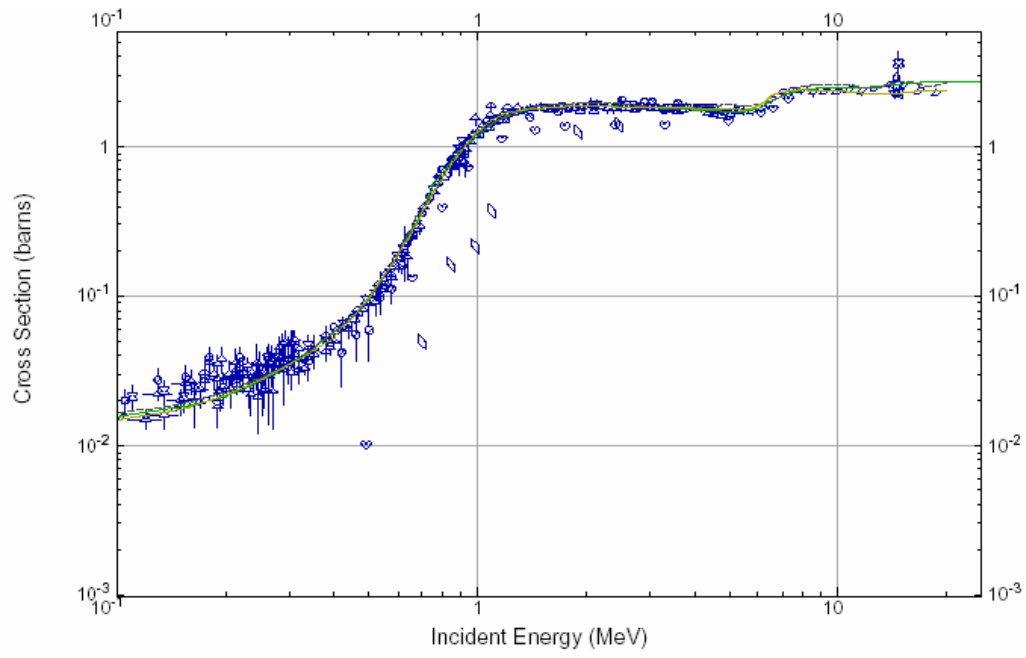


Figure A-5: fission cross section of  $^{241}\text{Am}$  in the high energy range.

# $^{243}\text{Am}(n,f)$

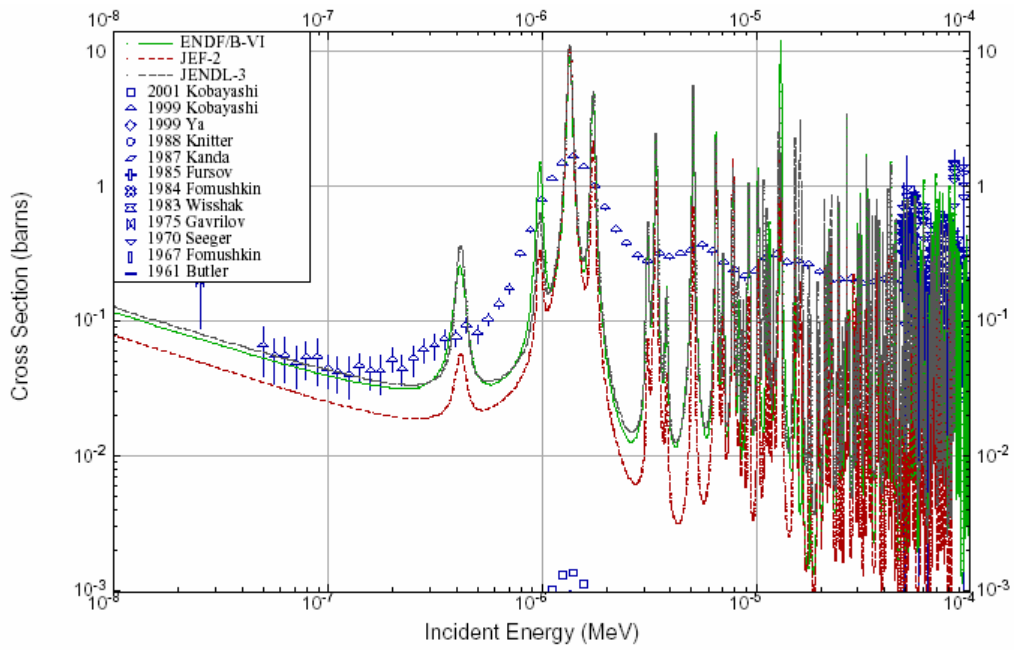


Figure A-6: fission cross section of  $^{243}\text{Am}$  in the low energy region.

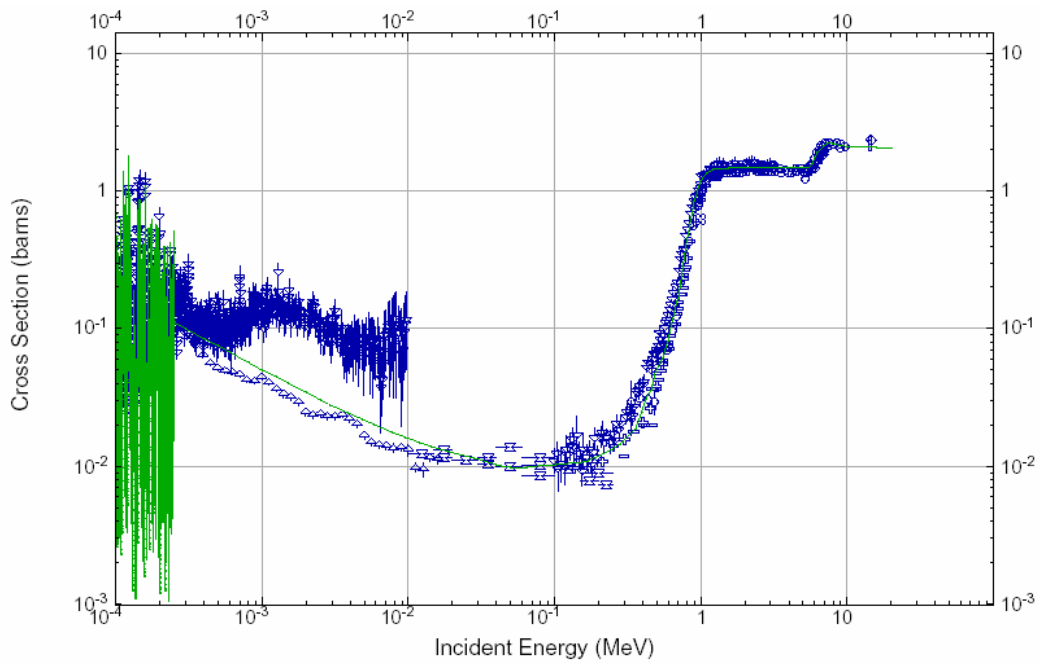


Figure A-7: fission cross section of  $^{243}\text{Am}$  in the high energy region.

# $^{245}\text{Cm}(n,f)$

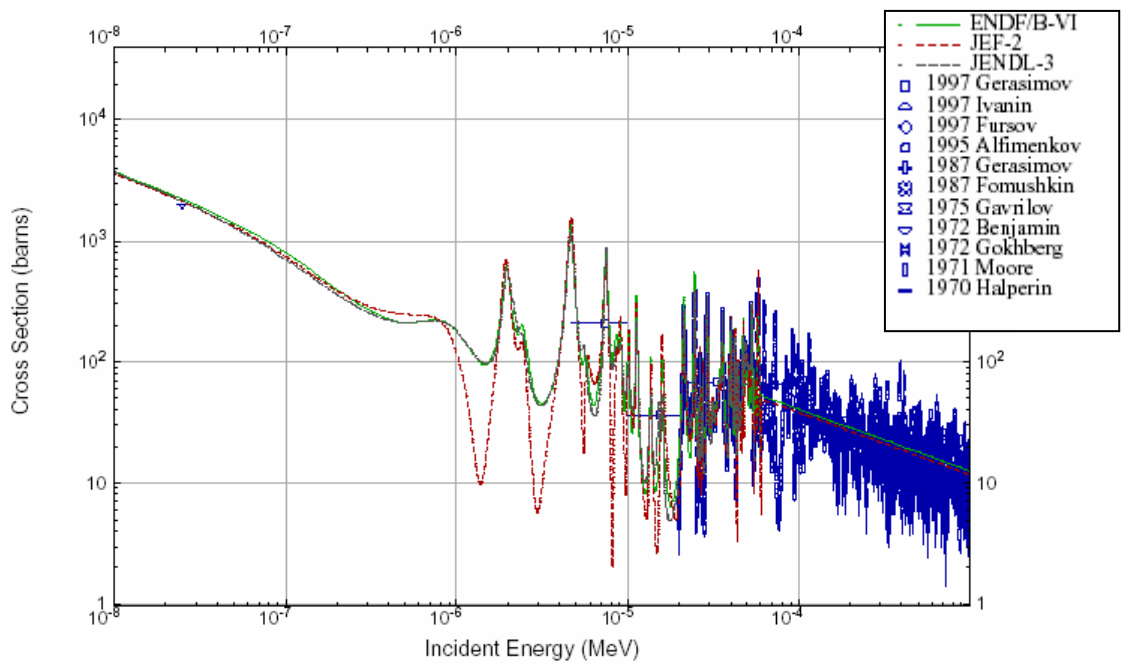


Figure A-8: fission cross section of  $^{245}\text{Cm}$  in the low energy region.

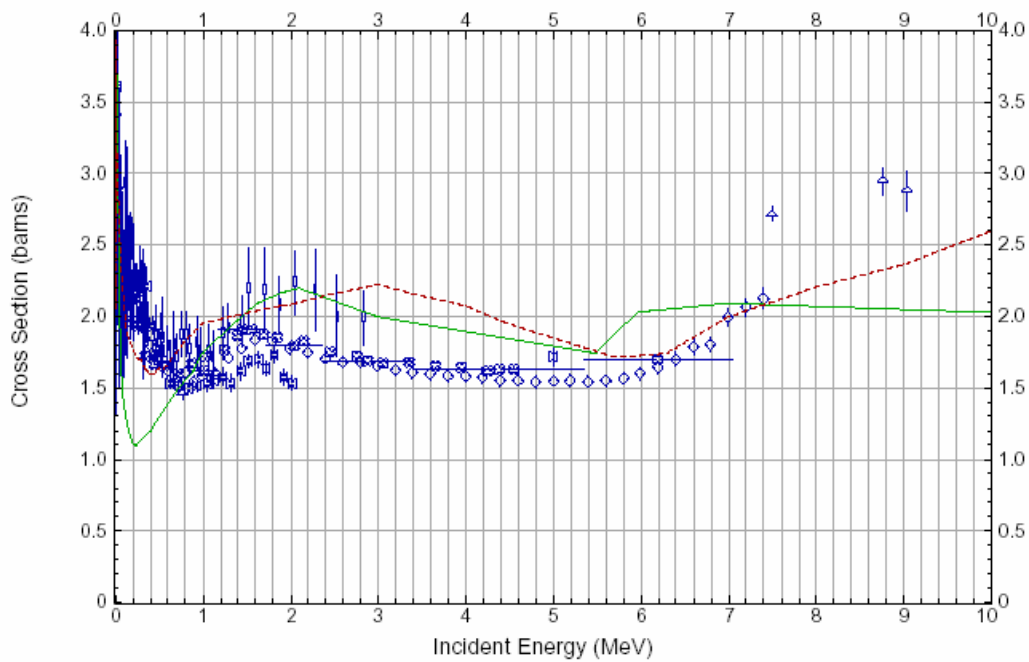


Figure A-9: fission cross section of  $^{245}\text{Cm}$  in the high energy region.

## References

---

- [1] C. Rubbia *et al.*, *Conceptual design of a fast Neutron Operated High Power Energy Amplifier*, CERN/AT/95-44(ET).
- [2] C. Rubbia *et al.*, *Nuclear Waste Burner (NWB) – an ADS Industrial Prototype for Minor Actinides Elimination*, n\_TOF Winter School, Centre de Physique de Les Houches, February 2003. Proceedings in press (2003).
- [3] E. Gonzalez *et al.*, *Applied physics measurements at the n\_TOF facility. Astrophysics, Symmetries, and Applied Physics at Spallation Neutron Sources*, ASAP 2002. World Scientific. ISBN 981-238-249-6 (2002).
- [4] The n\_TOF Collaboration, *CERN n\_TOF Facility: Performance Report*, INTC-2002-037.
- [5] EXFOR, *Experimental Nuclear Reaction Data File*.  
(see: [www-nds.iaea.org/at/exfor](http://www-nds.iaea.org/at/exfor))
- [6] A. Yamanaka *et al.*, *J. Nucl. Sci. Technol.*, **36** (1993) 863.
- [7] S. Plattard *et al.*, *Nucl. Sci. Eng.*, **61** (1976) 477.
- [8] A.D. Carlson *et al.*, in *Proc. Int. Conf. Nucl. Data for Science and Technology*, Gatlinberg, Tennessee, 1994, ANS, Vol.1, (1994), pag. 40.
- [9] C.D. Bowman *et al.*, *Phys. Rev.*, **137** (1965) B326.
- [10] P.A. Seeger *et al.*, *Nucl. Phys.*, A **96** (1967) 605.
- [11] W. Hage, K. Wisshak, and F. Käppeler, *Nucl. Sci. Eng.*, **78** (1981) 248.
- [12] K. Wisshak and F. Käppeler, *Nucl. Sci. Eng.*, **76** (1980) 148.
- [13] D.B. Gayther *et al.*, *Proc. Of the 4<sup>th</sup> All-Union Conf. On Neutron Phys.*, Kiev, Part 3, (1977) pag. 3.
- [14] J.W.T. Dabbs *et al.*, *Nucl. Sci. Eng.*, **83** (1983) 22.
- [15] H.H. Knitter *et al.*, *Atomkernerergie-Kerntechnik*, **33** (1979) 205.
- [16] J.W. Behrens and J. C. Browne, *Nucl. Sci.Eng.*, **77** (1981) 444.
- [17] M. Baba *et al.*, *J. Nucl. Sci. Technol.*, **38** (1989) 11.



- 
- [18] K. Kobayashi *et al.*, in Proc. Int. Conf. Nucl. Data for Science and Technology, Gatlinberg, Tennessee, 1994, ANS, Vol.1, (1994), pag. 242.
- [19] P.A. Seeger *et al.*, LA-4420 (LANL, 1970).
- [20] K. Wisshak *et al.*, Nucl. Sci. Eng., **85** (1983) 251.
- [21] H.H. Knitter *et al.*, Nucl. Sci. Eng., **99** (1988) 1.
- [22] Kobayashi *et al.*, in Proc. Int. Conf. Nucl. Data for Science and Technology, Trieste, Italy, 1997, SIF, Vol.59, Part 1, p. 638 (1997).
- [23] E.F. Fomushkin *et al.*, Atomic Energy, **242** (1987) 63.
- [24] R. White *et al.*, in Proc. Int. Conf. Nucl. Data for Science and Technology, Antwerpen, Belgium, 1982, Dardrecht, p. 218 (1983).
- [25] B.F. Fursov *et al.*, in Proc. Int. Conf. Nucl. Data for Science and Technology, Gatlinberg, Tennessee, 1994, ANS, Vol.1, p. 269 (1994).
- [26] I.A. Ivanin *et al.*, in Proc. Int. Conf. Nucl. Data for Science and Technology, Trieste, Italy, 1997, SIF, Vol.59, Part 1, p. 664 (1997).
- [27] V.F. Gerasimov *et al.*, in Proc. 5<sup>th</sup> Int. Seminar on interaction of Neutrons with Nuclei, ISINN-5, Dubna, p. 361 (1997).
- [28] F.Casagrande, P.Cennini, and X. Li, *The Argon Gas Detectors for the Fission Measurement in FEAT*. NIM in Physics Research A **372** (1996), pag. 307-310.
- [29] L. Zanini *et al.*, *Simulation of the FIC Detector*, AB-ATB Internal Note, (2003). In preparation.